THERMAL STRESSES IN A SINGLE ELASTIC FIBER EMBEDDED IN AN INFINITE MATRIX

I.E. ESPARRAGOZA*
School of Engineering Design, Technology and Professional Programs
The Pennsylvania State University
25 Yearsley Mill Rd., Media, PA 19063, USA
e-mail: iee1@psu.edu

C. LEVY and N.E. CAUDILL
Department of Mechanical and Materials Engineering
Florida International University
10555 W. Flagler St, Miami, FL 33174, USA

In this work, an analytical solution of the thermal stresses for a fiber embedded in a matrix is presented based on the idea of the boundary layer and under some simplifying assumptions. These assumptions include: the properties of both materials, fiber and matrix, remain constant; both materials remain in the elastic range so no plastic-deformation are considered; there exists a perfect bonding between the fiber and matrix so the condition of no-opening holds over the entire interface; and the composite is subjected to an uniform change of temperature. The analytical solution to the problem is found for the case when the length of the embedded bar (fiber) is much greater than its radius, and the Young's modulus of the matrix is much less than that of the fiber. The problem is also solved numerically by means of finite element analysis using a commercial package. Both results are compared and it is shown that both approaches coincide very close qualitatively and quantitatively although significant discrepancies may appear at specific points for specific cases.

Key words: fiber, thermal stresses, analytical approach, numerical analysis.

1. Introduction

One of the classical problems in unidirectional fibrous composites is due to the change in the temperature in the composite and the mismatch in the coefficient of thermal expansion of the fiber and matrix. Due to these two factors, thermal stresses develop in the composite and they are almost impossible to avoid. Temperature is a critical issue in composites and substantially influences all processes of deformation and fracture of composites as well as the physical and chemical properties of composites. The effect of temperature in the behavior of composites is a topic of major research. A list of publications (Parker *et al.*, 1961; Kerrish, 1971; 1972; Taylor, 1983; 1993; Koráb *et al.*, 2002; Greszczuk, 1965; Schapery, 1968; Wakashima *et al.*, 1974; Uemura and Yamaguchi, 1976; Ishikawa and Kobayashi, 1977) can be found for the study of the coefficient of thermal expansion in fibrous composites. However, these works are devoted to the macro-mechanics behavior of composites and the relation between the thermal expansion coefficient and the volume fraction of material composites.

Some papers can be found that include the temperature effect in the micromechanics analysis of fibrous composites. In Hseuh (1990) the effects of axial and radial residual stresses during pull-out as well as the debonding problem due to thermal residual stresses are studied. The pull-out problem of a fiber using a fracture mechanics approach which took into account residual stresses due to thermal cool-down is considered in Hutchinson and Jensen (1990). In Yeh and Krempl (1993) the vanishing fiber diameter with thermoviscoplasticity theory is introduced to analyze the effects of temperature rate on the residual stresses

* To whom correspondence should be addressed

when the unidirectional fibrous metal-matrix composite is cooled down during manufacturing. The transverse crack propagation in the fibers of composites due to thermal stresses is studied in Xu and Reifsnider (1994).

The shear lag theory (Cox, 1952), which is based entirely on elastic interactions, has also been used by many researchers to study the thermal stresses in fibrous composites. In Chawla (1987) the hygrothermal stresses in fibrous composites for the case of a central fiber surrounded by a shell of matrix are studied. This approach is similar to the one used in the shear-lag theory for low volume fractions and the stresses for the matrix sleeve are found. In Nairn (1997) the shear-lag theory is used to study the stress transfer in unidirectional composites. Here the most common shear-lag parameter is replaced by a new one derived from the approximate elasticity analysis. The prediction of the axial stress in the fiber and the total strain energy improved with the introduction of the new shear-lag parameter. In Landis and McMeeking (1998) and Beyerlein and Landis (1999) the foundations of the shear-lag theory was laid which was later used in Landis (2001) to predict the thermal stresses for the case of a periodic arrangement of unidirectional fibers. In Okabe and Takeda (2002) the elastoplastic shear-lag analysis is applied for a single-fiber composite. Here the three dimensional shear-lag analysis is used to predict the strength in unidirectional multi-fiber composites taking into account the temperature difference during the cure. More recently in Papanicolaou *et al*. (2002) and You (2003) the thermal stresses taking into account a transition layer along the interface between the fiber and matrix are studied.

Here in this work, the approach introduced in Cherepanov (1983) is used. This approach as well as the shear-lag theory is based on the equations of equilibrium between the fiber and matrix, the theory of elasticity and some simplifying assumptions. However, the main difference with respect to the shear-lag approach is the definition of a perturbed domain in the matrix close to the fiber interface, which determines the boundary layer region. The size of this region was proposed in Cherepanov (1983) and later used in the solution of other classical problems of fibrous composites in Cherepanov and Esparragoza (1995) and Esparragoza *et al*. (2003). This approach provides good results predicting the stresses and temperature distribution when compared to numerical results using the Finite Element Analysis (FEA). This approach works reasonably well for any stress level as well as for higher volume fractions in contrast to the shear lag theory that works only for low stresses. The use of the intuitive concept of boundary layer and the definition of the perturbed region close to the fiber makes this approach simple and unique. This is not only applicable to mechanical load (Cherepanov and Esparragoza, 1995) but also to thermal load as shown in this work.

2. Analytical approach

The problem under consideration consists of a round cylinder of finite length, the fiber, embedded in a linearly elastic infinite space of another material, the matrix, (Fig.1). Cylindrical coordinates are used where z is the axis of symmetry along the fiber length and r is the radial distance. Infinite here means that $z >> l$ and $r >> r_o$. The system is subjected to a constant change of temperature, ΔT.

The following designations will be used: r_o and l, radius and length of the embedded fiber; E_f and E_m, the Young's modulus of the fiber and matrix, respectively; ν_f and ν_m the Poisson's ratio of the fiber and matrix, respectively, and α_f and α_m the coefficient of thermal expansion of the fiber and matrix, respectively.

The thermal stresses in a fiber embedded in a matrix are studied based on the following assumptions: 1) the material properties of both materials, fiber and matrix, remain constant; 2) both materials remain in the elastic range so no plastic-deformation is considered; 3) a perfect bonding between the fiber and matrix exists, therefore, a condition of no fiber-matrix separation holds over the entire interface; and 4) the composite is subjected to an uniform change of temperature.

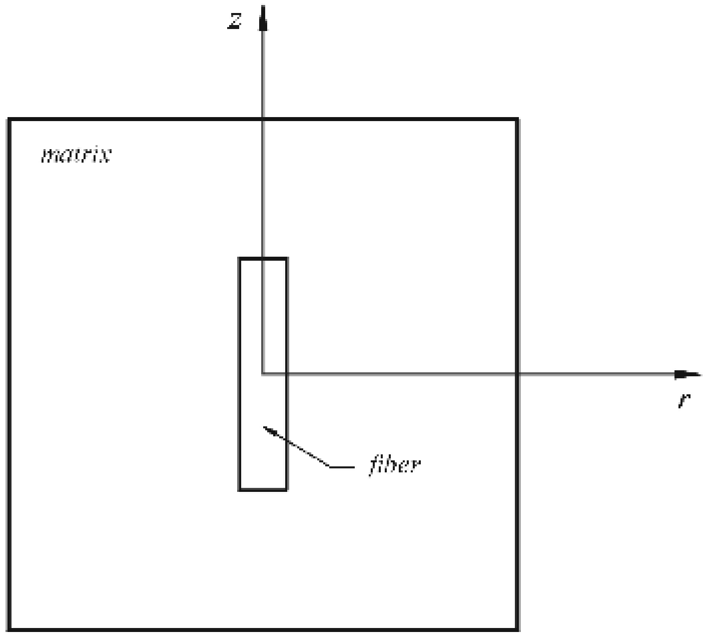

Fig.1. A fiber embedded in an infinite space of another material (matrix).

The following dimensionless quantities are introduced

$$\lambda = \frac{r_o}{l} \quad \text{and} \quad \beta = \frac{E_m}{E_f} . \tag{2.1}$$

Since it is assumed that perfect bonding exists between the fiber and the matrix, bonding between fiber and matrix is assumed to hold over the entire interface including the lateral surface and the ends.

The case when both λ and β are small is under study, i.e., when

$$\lambda = \frac{r_o}{l} << 1 \quad \text{and} \quad \beta = \frac{E_m}{E_f} << 1 . \tag{2.2}$$

It means that the radius of the fiber is much smaller than its length, and the elastic modulus of the thin fiber is much greater than the elastic modulus of the matrix. This is the case of most practical relevancy to composites.

Even though similar problems have been considered by other researchers, as mentioned before and cited in the references, their theoretical approaches are different to the one suggested here. Generally speaking, they do not take full advantage of the small ratio of λ and β. The use of the boundary layer concept to the solution of this problem, taking into account the small ratios described above, provides a means to obtain the necessary accuracy and conciseness for more difficult cases. This is to say, the size of the matrix suggested by other authors and based on a periodic arrangement of fibers is replaced here by a perturbed region on an infinite matrix. The analytical approach suggested here is based on the ideas proposed in Cherepanov (1983).

The problem can be modeled as a round cylinder of finite length embedded in a linearly elastic half-space of another material as shown in Fig.2. Here, both fiber and matrix are analyzed in detail considering the equilibrium and boundary conditions governing the problem.

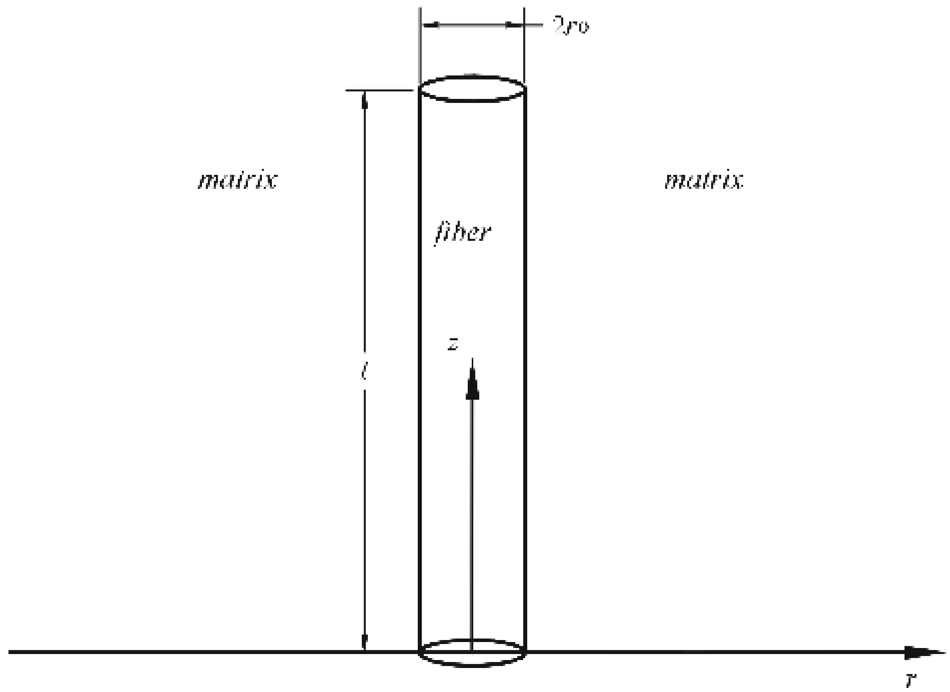

Fig.2. Thin fiber embedded in an infinite space of another material.

Fiber:

In the case $\lambda << 1$ under study, the approximate analytical solution suggested in Cherepanov (1983) is used. According to this approach the displacement and stress-strain field in the fiber is described by the following three functions: $\sigma_f = \sigma_f(z)$ is the mean normal stress, σ_z, in a cross-section of the fiber; $\tau_f = \tau_f(z)$ is the mean shearing stress, τ_{rz}, on the lateral surface of the fiber; and $w_f = w_f(z)$ is the mean displacement of a cross-section of the fiber along the *z*-axis.

Using the differential control volume shown in Fig.3, the equilibrium equation states

$$\frac{d\sigma_f(z)}{dz} + \frac{2}{r_o}\tau_f(z) = 0. \tag{2.3}$$

From Hooke's law, taking into account thermal strains, it follows that

$$\varepsilon_f(z) = \frac{dw_f(z)}{dz} = \frac{\sigma_f(z)}{E_f} + \alpha_f \Delta T \tag{2.4}$$

where α_f and E_f are the coefficient of thermal expansion and Young's modulus of the fiber, respectively.

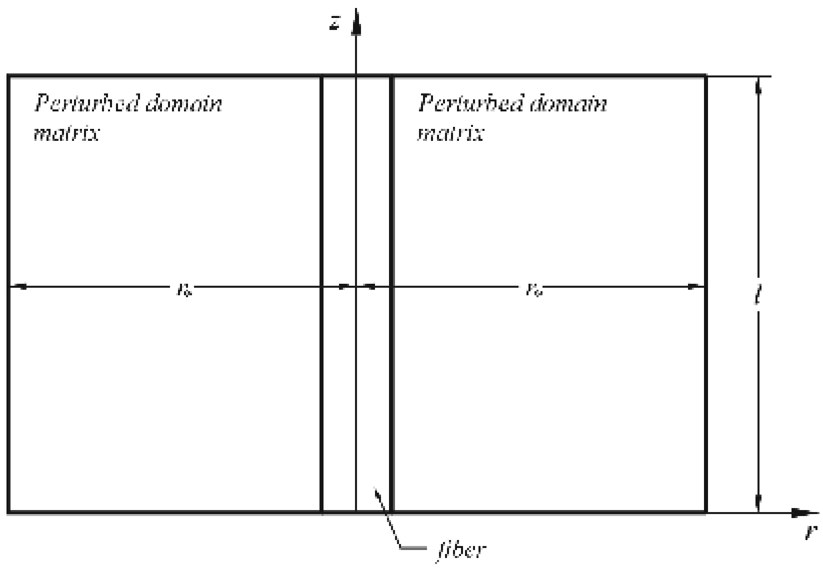

Fig.3. The cylindrical domain of a non zero perturbed field. Inside this domain the temperature in the matrix is a function of *r* and *z*; outside this domain, the temperature of the matrix is a function of *z* only.

Matrix:

Following the same approach, the perturbed field of stresses, strains and displacements in the matrix exist only inside the perturbed region close to the fiber. This region is determined by the cylindrical domain of perturbation D_p defined by radius r_* (Cherepanov and Esparragoza, 1995) (Fig.3). Generally, r_*, is a function of *z*, but is taken constant in this study (Cherepanov and Esparragoza, 1995). This assumption is satisfactorily confirmed by the numerical experiments.

In this problem both the fiber and the domain of perturbation in the matrix are assumed to be round cylinders. Thus the problem is axisymmetric with *z* as the axis of symmetry and *r* is the radial distance from the axis.

Inside this cylindrical domain $D_p(r_o < r < r_*,\ 0 < z < l)$, the fields of stresses strain and displacement are described by the following three functions: $w_m = w_m(r, z)$, is the *z* component of the displacement vector; $\sigma_m = \sigma_m(r, z)$ and $\tau_m = \tau_m(r, z)$ are the respective components σ_z and τ_{rz} of the stress tensor. All other components of the stress tensor and displacement vector are considered small enough to be neglected.

Inside the cylindrical perturbed domain the following equations are assumed to be valid

From equilibrium:

$$\frac{\partial}{\partial r}[r\tau_m(r, z)] + r\frac{\partial\sigma_m(r, z)}{\partial z} = 0 . \tag{2.5}$$

From Hooke's law

$$\tau_m(r, z) = G_m\gamma = G_m\left(\frac{\partial w_m}{\partial r} + \frac{\partial v_m}{\partial z}\right) \tag{2.6}$$

where, $v_m = v_m(r, z)$, is the displacement in the *r*-direction, G_m is the matrix shear modulus and γ is the engineering shear stress γ_{rz}.

Since the problem under study is for $\lambda << 1$, the stress field around the fiber has a boundary layer like the structure of Cherepanov (1983). In this case, the gradients across the *r*-direction are much greater than the gradients along the *z*-direction. Therefore, Eqs (2.5) and (2.6) might be reduced to the form

$$\frac{\partial}{\partial r}\left[r\tau_m(r, z)\right] = 0 \tag{2.7}$$

and

$$\tau_m(r, z) = G_m \frac{\partial w_m(r, z)}{\partial r}. \tag{2.8}$$

Also in the matrix but outside the perturbed region $(r > r_*)$, the axial displacement of the matrix and the axial strain might be assumed to be a function of *z* only. Therefore, Hooke's law, taking into account thermal strains, can be written as follows

$$\varepsilon_m = \varepsilon_m(z) = \frac{dw_m}{dz} = \alpha_m \Delta T \tag{2.9}$$

where α_m is the coefficient of thermal expansion of the matrix.

Boundary Conditions:

The conditions of equilibrium and bonding at the interface are

at $\quad r = r_o, \quad \tau_f(z) = \tau_m(r, z),$ (2.10)

at $\quad r = r_o, \quad w_f(z) = w_m(r, z).$ (2.11)

The condition of displacement continuity at the boundary of the perturbed domain is

at $\quad r = r_*, \quad w_m(r, z) = w_m(z).$ (2.12)

Since the problem has a plane of symmetry at the *z* axis, it can be reduced to solving a half space problem. This leads to the condition of no-displacement at the plane $z = 0$ outside the perturbed domain to be

for $\quad r > r_* \quad$ at $\quad z = 0, \quad w_m(z) = 0.$ (2.13)

The system of Eqs (2.3) to (2.13) totally describes the approach undertaken to find the approximate analytical solution to the problem under consideration. A detailed analytical approach can be found in (Esparragoza and Caudill (2003). The final solution for the normal thermal stress along the fiber is given by

$$\sigma_f(z) = E_f\left(\alpha_f - \alpha_m\right)\Delta T\left[\frac{\cosh\left(\frac{k}{l}z\right)}{\cosh(k)} - 1\right] \tag{2.14}$$

and the solution for the shearing stress is given by

$$\tau_f(z) = -\left(\lambda \frac{k}{2}\right) E_f \left(\alpha_f - \alpha_m\right) \Delta T \left[\frac{\sinh\left(\frac{k}{l} z\right)}{\cosh(k)} \right] \tag{2.15}$$

where

$$k^2 = \frac{\beta}{\lambda^2 (1 + \nu_m) \ln \frac{r_*}{r_o}} . \tag{2.16}$$

Here, the perturbed domain radius, r_*, can be determined by

$$\frac{r_*}{r_o} = \left(\frac{l}{r_o}\right)^{\alpha} \tag{2.17}$$

where α is a fitting parameter suggested in Cherepanov (1983), where details about this parameter can be found, and used in Cherepanov and Esparragoza and Esparragoza *et al.* (2003). Additionally, the numerical experiments confirm well the analytical solution if the value of α is taken equal to Cherepanov (1983)

$$\alpha = 0.738 . \tag{2.18}$$

3. Numerical analysis

The computational numerical analysis is performed by means of the Finite Element Analysis using ANSYS version 5.7. Taking advantage of the axisymmetric condition of the problem, as well as its symmetry along $z = 0$, the ANSYS model is reduced from its full geometry, Fig.4, to a one quarter size of its original geometry as shown in Fig.5, without compromising the results.

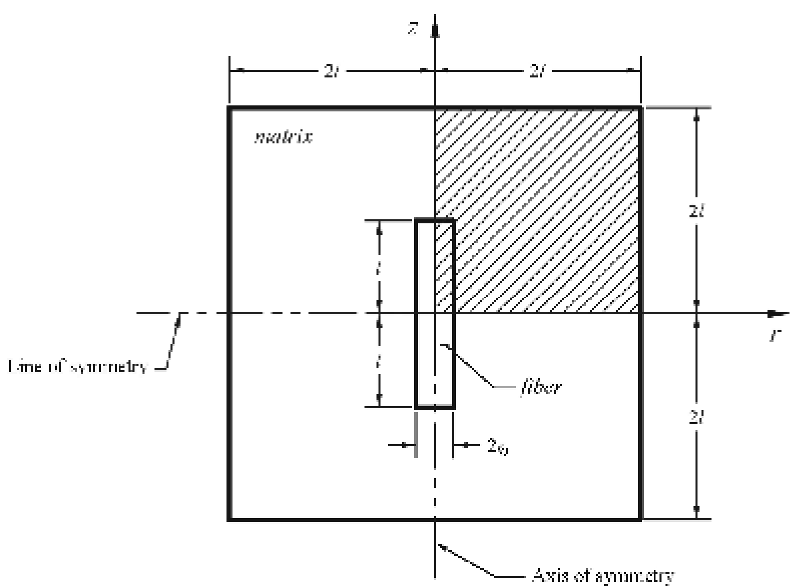

Fig.4. Geometric description of the fiber of length $2l$ embedded in an infinite matrix ($2l >> r_o$).

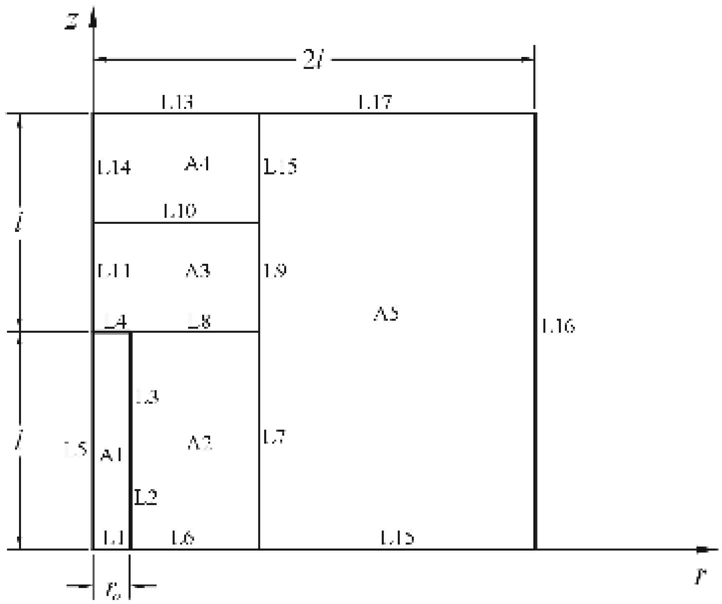

Fig.5. Geometry of the axisymmetric problem modeled in ANSYS.

The creation of areas *A2*, *A3*, and *A4* as shown in Fig.5 was not necessary, since there were only two materials; however they allowed creating a mapped mesh with full control of elements' size and quantity providing a better transition of elements between the interface of the fiber and matrix, where the stresses are of greater importance. With the completion of the geometry creation phase, now the material properties were assigned to the areas. Area A1 was attributed with the properties of material 1, the fiber, while areas *A2*, *A3*, *A4* and *A5* got the properties of material 2, the matrix. The different cases considered here were the result of varying the material properties, ratio $\beta = E_m / E_f$, and the radial dimensions of the fiber, ratio $\lambda = r_o / l$. Eight nodded quadrilateral elements were used that could serve for plane stress or strain, or for axisymmetric conditions. The respective options were set to Axisymmetric, Nodal stress and No extra output. The unit for temperature was set to Celsius degrees for all the cases studied.

In this work, the only necessary load is the change in temperature, ΔT . This was achieved by setting the uniform temperature, and reference temperature. The appropriate displacement constraints were applied next. The problem was solved numerically and the results are based on the average normal stresses at a cross-section along the fiber and the shear stresses at the interface.

The solution to any FEA problem could not be considered as an accurate representation of a physical or engineering problem without knowing that the mesh forming the elements of the model is small enough to capture the effect of its constraints and boundary conditions. This is known as convergence. In this work, checking convergence of the mesh in the model was performed by running the ANSYS model with a predetermined number of elements, monitoring the final displacement at one point in the fiber and at one point in the matrix, then running the same model again with a smaller mesh size, and comparing the displacement of both points. This process was repeated until convergence, no significant change in the displacement, was attained. Convergence was check for all the ANSYS models solved in this work to ensure accurate results.

4. Comparison of analytical and numerical results

The comparison is based on the normal and shearing stress distribution along the fiber. The analytical results come directly from Eqs (2.14) and (2.15). The numerical results were obtained using the finite element analysis results from ANSYS. Different cases were considered as a result of varying the material properties, ratio $\beta = E_m/E_f$, and the radial dimensions of the fiber, ratio $\lambda = r_o/l$. Figures 6 to 11 compared the numerical and analytical results of the normalized residual axial and interfacial shear stresses.

It is observed that the numerical results showed the same qualitative behavior of the analytical solution, serving as a validation tool against lack of experimental results. There was a large discrepancy in the results as the ratio z/l approached one. This is attributed to two reasons. The first one is that the analytical solution considered the axial stress at $z/l = 1$ small enough to be assumed zero; however, in the numerical analysis is observed that the axial stress at $z/l = 1$ is very small but not necessary zero. Therefore, there exists a small discrepancy in the stresses between the numerical and analytical solution mainly when z/l approaches one. This fact is especially seen in the case of short fiber aspect ratio. The second reason for the discrepancy in the results at the end is due to a singularity. Singularities occur at locations where a drastic transition in geometry or a difference in the properties of the materials is present. The best way to deal with this is by increasing the number of elements particularly in the affected region or by using singular elements in the finite element model. The latter approach has been used in fracture mechanics to determine the stress intensity factor at the crack tip. The approach used in this work was to increase the mesh size in the fiber and in the matrix, especially at the area close to the interface, so the discretization was maximized not only at the tip but along the whole interface. Then the results at the tip were simply discarded, knowing that the erratic behavior was already expected. This erratic behavior was observed around the last three percent of the fiber's length, close to $z/l = 1$, and was particularly noticed in the shear stress numerical results rather than in the axial stress. This was also expected since the shear stress was obtained from a single nodal value at the interface, while the axial stress was the result of the average across the fiber radius.

The percentage of error decreased as β decreased typically for longer fibers. This was especially observed for the interfacial shear stress error. As β decreased from *0.01* and *0.001* the maximum error decreased from fifty to the low twenty percent for the case when $\lambda = 0.005$ (see Figs 6 to 9). This agreed with the initial assumption of using e much less than unity. Figures 10, and 11, are for the case when $\lambda = 0.01$ and $\beta = 0.001$.

One of the difficulties in establishing the equations for the behavior of the residual stresses due to the difference in the coefficient of thermal expansion in a fiber embedded in an infinite matrix is that the radius of the perturbed region is not actually known. For the case when multiple fibers are present, the ratio of the perturbed radius to the fiber's radius could be related to the fiber volume fraction. Still the optimum value for the distance between fibers is unknown. Equations (2.17) and (2.18) have proven satisfactory in approximating the perturbed region in this work and in similar type of problems (Cherepanov and Esparragoza and Esparragoza *et al.*, 2003). They provided a good qualitative solution to the residual embedded in a soft material. This stresses when compared to the numerical solution from ANSYS. This applied to all conditions; short or long fiber embedded in a soft matrix, and short or long fiber embedded in a stiff matrix. However, the best agreement between the analytical and numerical solutions occurred for the case modeling a long fiber validated the original assumption of taking $\lambda << 1$ and $\beta << 1$. The error for the problem when $\lambda = 0.005$ and $\beta = 0.001$ started at around two percent in the axial stress at $z/l = 0$, stayed within five percent through $z/l = 0.6$, then increased to ten percent at $z/l = 0.75$, twenty percent at $z/l = 0.85$ and continued increasing to the end of the fiber. The shear stress started around twenty percent at $z/l = 0$, continued decreasing to less than one percent at $z/l = 0.9$, then increased again to the end. The reason for the discrepancies in the stresses as the end of the fiber is reached was discussed earlier.

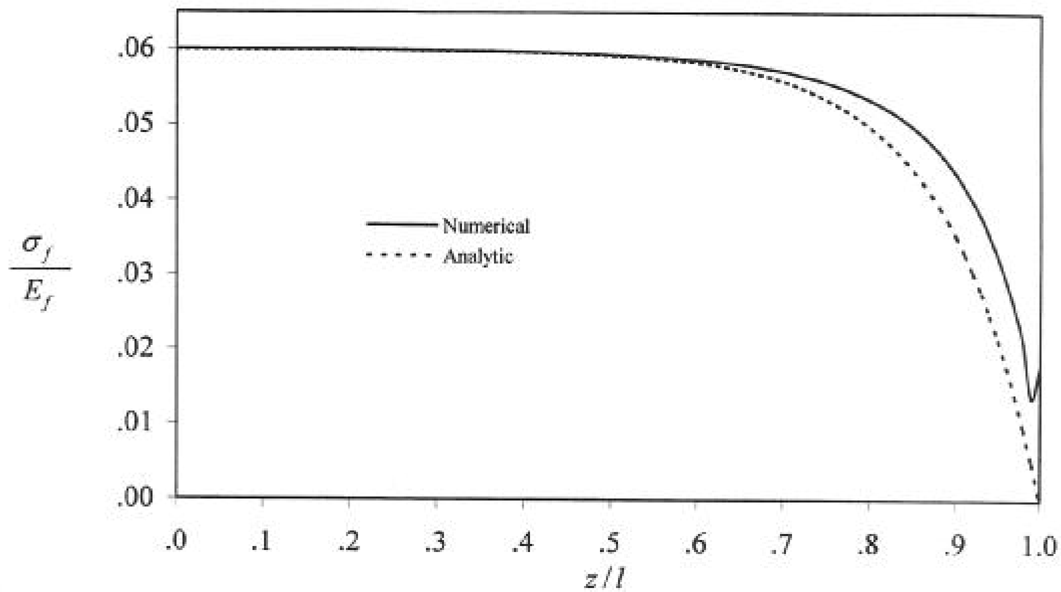

Fig.6. Comparison of normalized axial stress for $\lambda = 0.005$, $\beta = 0.01$, $\alpha_f - \alpha_m = -100e^{-6}\, 1/{}^{0}C$, $\Delta T = 600^{0}C$.

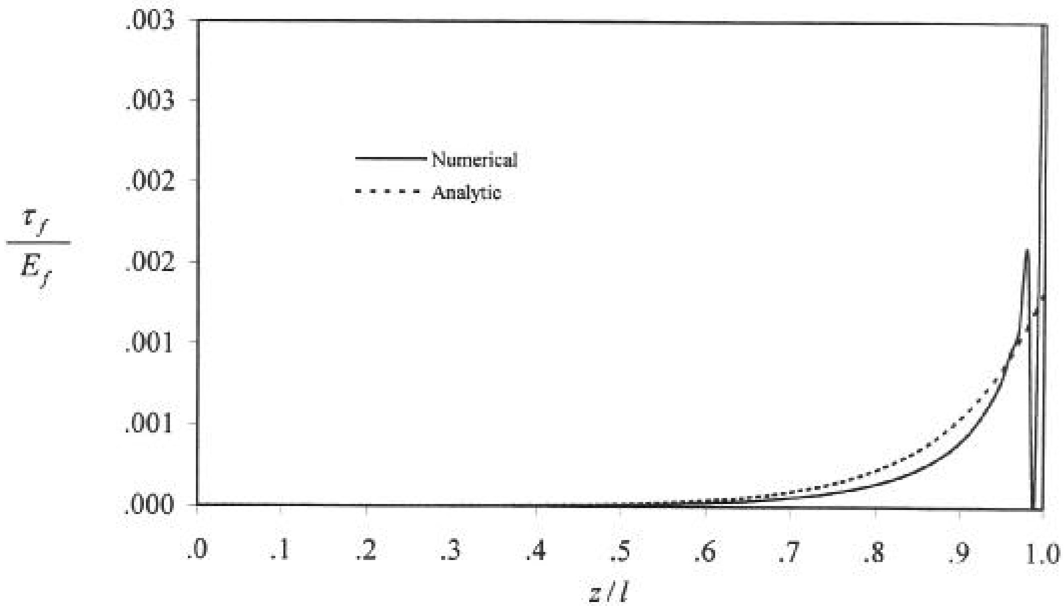

Fig.7. Comparison of normalized shear stress for $\lambda = 0.005$, $\beta = 0.01$, $\alpha_f - \alpha_m = -100e^{-6}\, 1/{}^{0}C$, $\Delta T = 600^{0}C$.

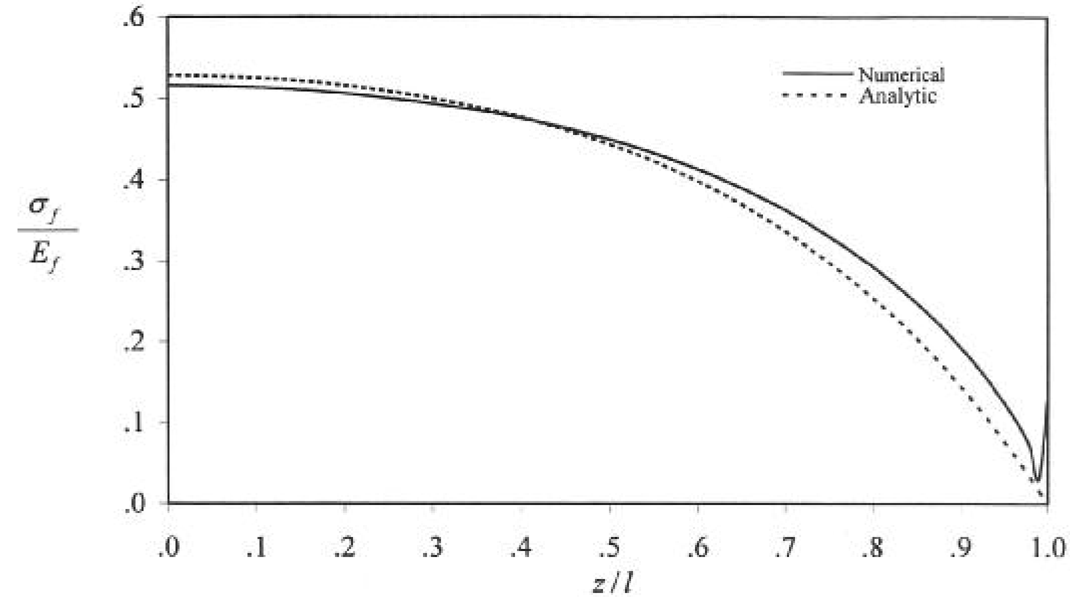

Fig.8. Comparison of normalized axial stress for $\lambda = 0.005$, $\beta = 0.001$, $\alpha_f - \alpha_m = -100e^{-6}\,1/{}^{0}C$, $\Delta T = 600^{0}C$.

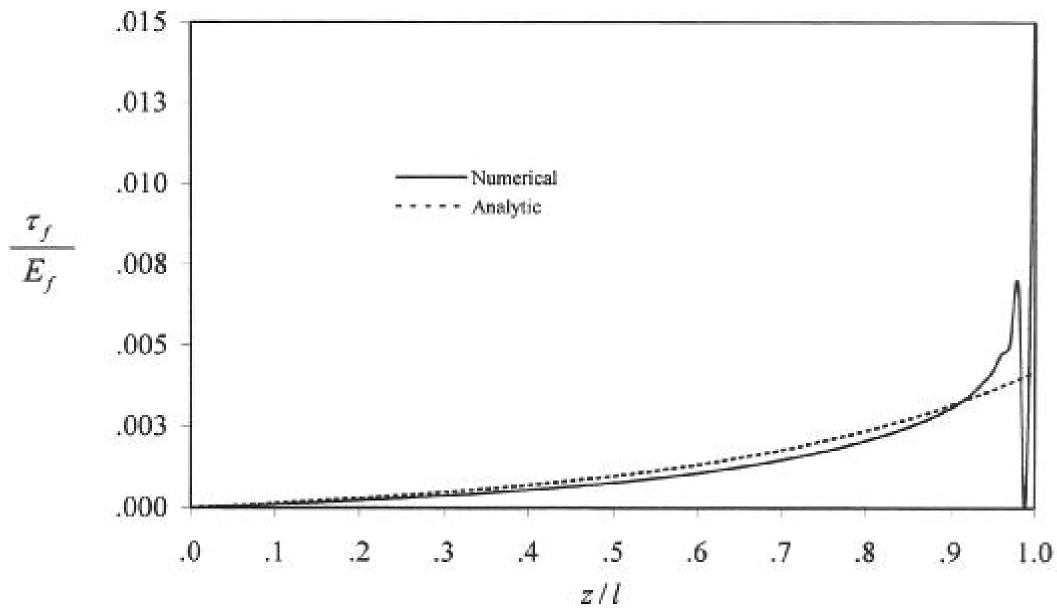

Fig.9. Comparison of normalized shear stress for $\lambda = 0.005$, $\beta = 0.001$, $\alpha_f - \alpha_m = -100e^{-6}\,1/{}^{0}C$, $\Delta T = 600^{0}C$.

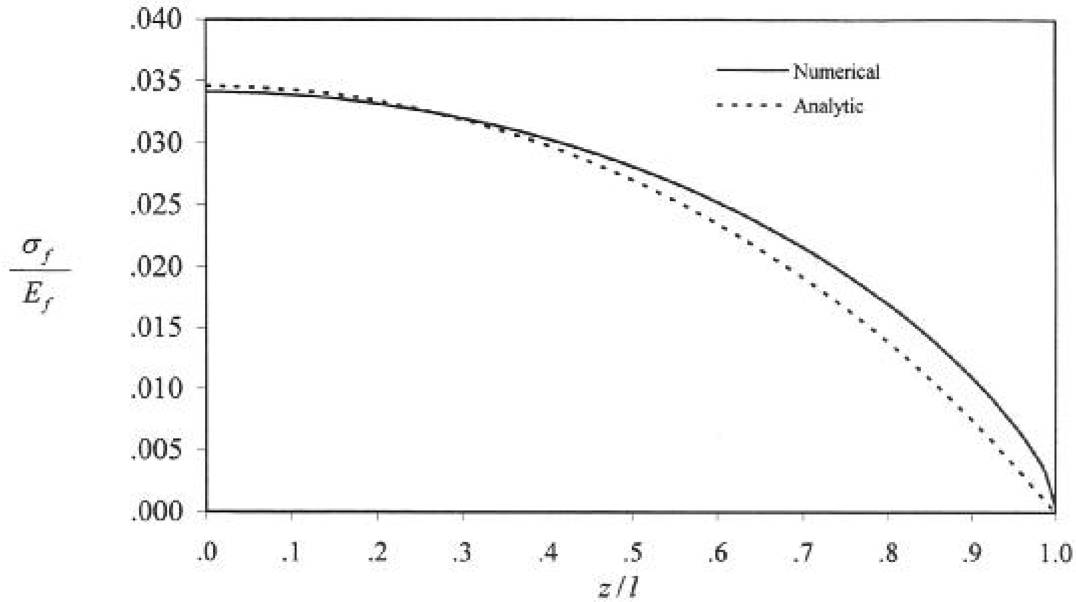

Fig.10. Comparison of normalized axial stress for $\lambda = 0.01$, $\beta = 0.001$, $\alpha_f - \alpha_m = -100e^{-6}\, 1/{}^{0}C$, $\Delta T = 600^{0}C$.

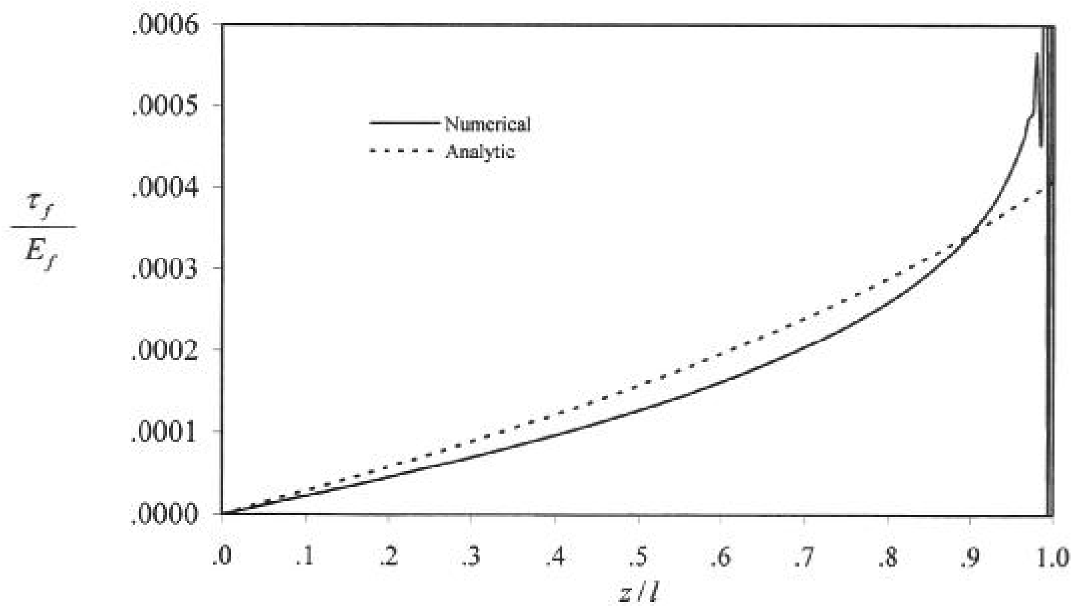

Fig.11. Comparison of normalized shear stress for $\lambda = 0.01$, $\beta = 0.001$, $\alpha_f - \alpha_m = -100e^{-6}\, 1/{}^{0}C$, $\Delta T = 600^{0}C$.

5. Conclusions

The numerical analysis confirmed the approximate analytical solution to the thermal stress along a fiber embedded in a matrix as presented in this paper. It is observed that the accuracy of coincidence of both results depends on the dimensionless ratios $\lambda = r_o/l$ and $\beta = E_m/E_f$. However, both approaches coincide qualitatively and quantitatively, even though substantial discrepancies might appear at particular points mainly due to the strong singularity present on this type of problem. Additionally, some of the discrepancies are due to the assumptions in the analytical model and the approximations involved in the numerical approach. It is recommended that experimental results be obtained to establish the real error and the limits of applicability of the approaches studied.

This work provides a simple method to determine the thermal stresses along the fiber embedded in a matrix based on some simplifying assumptions, setting the foundation for a better understanding of the interaction between the fiber and matrix in the case of the classical problem of thermal stresses. Furthermore, it also provides a new means to solve other related problems such as the residual thermal stress problem, the effect of temperature expansion during the debonding process, and the most complex problem of mechanical and thermal stresses in a fiber reinforced composite.

It is also of interest to determine the actual perturbed region in the matrix during the stress transfer. Users of the shear-lag theory have modified the shear lag parameter in order to model some specific problems. Here, the perturbed domain proposed in Cherepanov (1983) has been used obtaining very good results. However, more analysis of this perturbed region is necessary since it is evident that its size is not only a function of z but also a function of the materials properties and the dimensions of the embedded fiber. This idea lends itself to study the interaction between multiple fibers in a matrix. Once the perturbed domain is clearly defined and understood, the next step would be to study the interaction between two or more fibers, finding an expression for the optimal distance of the perturbed region that produces the best representation of the stress transfer between them. These topics will be discussed in future work.

Nomenclature

D_p – cylindrical domain of perturbation in the matrix
E_f – Young’s modulus of the fiber
E_m – Young’s modulus of the matrix
G_m – matrix shear modulus
k – dimensionless parameter
l – length of the embedded fiber
r – radial distance
r_o – radius of the fiber
r_* – radius of the perturbed region in the matrix
w_f – mean displacement of a cross-section of the fiber along the z-axis.
w_m – z component of the displacement vector in the matrix
z – axis of symmetry along the fiber length
α – fitting parameter
α_f – coefficient of thermal expansion of the fiber
α_m – coefficient of thermal expansion of the matrix
β – dimensionless parameter relating the Young’s modulus of the finer and matrix
γ – engineering shear stress in the matrix
ΔT – change of temperature
l – dimensionless parameter relating the radius and the embedded length of the fiber
ν_f – Poisson’s ratio of the fiber

ν_m – Poisson's ratio of the matrix
v_m – displacement in the *r*-direction in the matrix
σ_f – mean normal stress in a cross-section of the fiber
σ_m – normal stress component of the stress tensor in the matrix
τ_f – mean shearing stress on the lateral surface of the fiber
τ_m – shearing stress component of the stress tensor in the matrix

References

Beyerlein I.J. and Landis C.M. (1999): *Shear-lag model for failure simulations of unidirectional fiber composites including matrix stiffness.* – Mech. Mat., vol.31, No.5, pp.331-350.

Chawla K.K. (1987): *Composite Materials. – Science and Engineering.* – Springer-Verlag.

Cherepanov G.P. (1983): *Fracture Mechanics of Composites* (In Russian). – Moscow: Nauka Publisher.

Cherepanov G.P. and Esparragoza I.E. (1995): *The problem of fiber pullout.* – Mat. Sci. and Engineering A, vol.203, pp.332-342.

Cox H.L. (1952): *The elasticity and strength of paper and other fibrous materials.* – British Journal of Applied Physics, vol.3, pp.72-79.

Esparragoza I.E. and Caudill N. (2003): *On the theory of the thermal stresses in a fiber embedded in a matrix.* – Proceedings of the 5th International Congress of Thermal Stresses and Related Topics, TS2003, 8-11 June 2003, Blacksburg, VA, MM-5-2-1, MM-5-2-4.

Esparragoza I.E., Aziz A.H. and Damle A.S. (2003): *Temperature distribution along a fiber embedded in matrix under steady state conditions.* – Composites: Part B, vol.34, pp.429-436.

Greszczuk L.B. (1965): *Thermoelastic properties of filamentary composites.* – Proceedings AIAA 6th Struct. Mat. Conference :285.

Hseuh C.H. (1990): *Interfacial debonding and fiber pull-out stresses of fiber reinforced composites.* – J. Mat. Sci. and Eng., vol.A123, pp.1-11.

Hutchinson J.W. and Jensen H.M. (1990): *Models of fiber debonding and pull-out in brittle composites with friction.* – Mech. Mat., vol.9, pp.139-163.

Ishikawa T. and Kobayashi S. (1977): *Thermal expansion coefficients of unidirectional fiber reinforced composites.* – J. Jpn. Soc. Aeronaut. Space Sci., vol.25, Part 1, pp.394-400, Part 2, pp.423-429.

Kerrish J.F. (9171): *Thermal diffusivity of heterogeneous materials.* – J. Appl. Phys., vol.42, pp.267-271.

Kerrish J.F. (1972): *Thermal diffusivity of heterogeneous materials. II. Limits of steady-state approximation.* – J. Appl. Phys., vol.43, pp.112-117.

Koráb J., Štefánik P., Kavecký Š., Šebo P. and Korb G. (2002): *Thermal conductivity of unidirectional copper matrix carbon fibre composites.* – Composites Part A., vol.33, pp.577-581.

Landis C.M. (2001): *Shear lag modeling of thermal stresses in unidirectional composites.* – Proceedings of the 10th International Conference on Fracture, Ref. ICF100374OR.

Landis C.M. and McMeeking R.M. (1998): *Stress concentrations in composites with interface sliding, matrix stiffness, and uneven fiber spacing using shear-lag theory.* – Int. J. Solid Struc., vol.36, pp.4333-4361.

Nairn J.A. (1997): *On the use of shear-lag methods for analysis of stress transfer in unidirectional composites.* – Mech. Mat., vol.26, pp.63-80.

Okabe T. and Takeda N. (2002): *Elastoplastic shear-lag analysis of single-fiber composites and strength prediction of unidirectional multi-fiber composites.* – Composites: Part A, vol.33, pp.1327-1335.

Papanicolaou G.C., Michalopoulou M.V. and Anifantis N.K. (2002): *Thermal stresses in fibrous composites incorporating hybrid interphase regions.* – Comp. Sci. and Tech., vol.62, pp.1881-1894.

Parker W.J., Jenkins R.J. and Abbott G.L. (1961): *Thermal diffusivity of measurement using the flash technique*. – J. Appl. Phys., vol.32, pp.1679-1684.

Schapery R.A. (1968): *Thermal expansion coefficients of composite materials based on energy principle*. – J. Comp. Materials. vol.2, pp.380-404.

Taylor R.E. (1983): *Thermal diffusivity of composites*. – 8ETPC Proceedings of High Temperatures-High Pressures, vol.15, pp.299-309.

Taylor R.E. (1993): *Thermal conductivity of carbon fibers*. – Proceedings of High Temperatures-High Pressures. vol.25, pp.443-450.

Uemura M. and Yamaguchi Y. (1976*): Thermal expansion coefficients and residual stresses in filament-wound CFRP materials*. – 5th FRP Symp. Jpn. Soc. Mater. Sci., pp.38-41.

Wakashima K., Otsuka M. and Umekawa S. (1974): *Thermal expansions of heterogeneous solids containing aligned ellipsoidal inclusions*. – J. Comp. Materials., vol.8, pp.391-404.

Xu Y.L. and Reifsnider K.L. (1994): *Micromechanical analysis of fiber crack propagation in fibrous composites due to thermal stresses*. – J. Thermal Stresses, vol.17, pp.143-161.

Yeh N.M. and Krempl E. (1993): *Influence of cool-down temperature histories on the residual stresses in fibrous metal-matrix composites*. – J. Comp. Materials, vol.27, No.10, pp.973-995.

You L.H. (2003): *Thermal stress distributions in axisymmetrical orthotropic fiber-reinforced composites with multilayered interfaces*. – J. Mats. Sci., vol.38, No.13, pp.2963-2970.

Received: July 6, 2005

Revised: October 19, 2005